AN ITERATIVE SOLUTION OF THE INVERSE GRAVITY PROBLEM FOR CONSTRAINED MODELS

by

A. MESKÓ

Department of Geophysics, Eötvös University, Budapest
Received: 15 March 1975

SUMMARY

An iterative solution of the inverse gravity problem is described in the case where the gravity field is due to the undulation of the interface between two layers with different densities. The method proposed here consists of setting up a starter model computing the gravity field due to the model and modifying the model in an iterative manner until a good approximation between measured and computed gravity fields is obtained. The method resembles to the procedure described by Cordell and Henderson (1968) but the computation of the gravity field is simplified and the corrections to be applied in due course of the iterations are determined more efficiently. As a result the number of iterations, necessary to achieve a given accuracy, are significantly decreased as well as the computer time required by the process.

The accuracy of the approximations used in the computation of the gravity field due to the model are investigated in Part I. and Part II. The iterative process and examples of its applications are described in Part III.

Introduction

The purpose of this paper is to describe an economical algorithm for solving the inverse gravity problem in the simplified but practically useful case when the gravity anomalies are due to a single density contrast. Most methods known form the literature (Cordell and Henderson 1968, M. Al-Chalabi 1971 etc.) set up a geological model, specify some of its parameters and then determine the other parameters by using some sort of iterative or optimization algorithm. The objective is to compute or modify in each step the free or adjustable parameters in such a way that the gravity anomaly, produced by the structural model possessing these parameters be close to the measured gravity anomalies. The fit between the computed and measured data may be considered complete if the differences do not exceed the measurement errors. Some other criterion may also be used to express the goodness of fit between the two sets of data. No author claimed that a unique solution can be reached. An appropriate selection of the adjustable parameters (in most cases the density contrast and the depth of the lower or upper surface of the anomalous bodies), however, could yield geologically feasible solutions. This solution, even if the required goodness of fit has been arrived, still may be incorrect because some additional assumptions

have to be valid e.g. there should be no more than a single density contrast and its maximum depth should be given to a good approximation, regional background and random errors must not exceed an upper limit etc. Feasible models, however, do help the interpretation even if they have obvious limitations and contribute to a better understanding of the prospected area. Therefore it is hoped that the solution of the inverse gravity problem as proposed in the present paper may be of interest.

The iterative solution, described in detail in Part 3. is a modification of the method by Cordell and Henderson (1968). Modifications became necessary because the original version needs too large an amount of computer time. 20 iterations for 20×20 data array run 9,0 minutes on an IBM 360/65 computer (Cordell – Henderson 1968 p. 598). Solutions, obtained by different approaches require also too large computer times.

We have to work on larger data array and the computers available to us are slower than those mentioned in the cited publication. The computation of the gravity field due to the model had to be simplified and the convergence of the iterative process had to be made faster.

Gravity fields due to irregularly shaped bodies are usually obtained by dividing the bodies into rectangular prisms and adding up the effects of these elements (e.g. Nagy 1966). Some authors (e.g. Botezatu et al 1971) suggest the use of cubes. The gravity field of rectangular prisms can be given analytically. Various expressions are known from the literature (Nagy 1966, Goodacre 1973 etc.) none of these is easy to handle. Long and tedious computations are involved the repeated use of which in each iterative step for all observation points requires so much computer time that practically prohibits the use of the exact formula. In its stead we approximate the fields of rectangular prisms by fields of mass points. The masses are equal to the mass of the corresponding prisms and all points lie in a horizontal plane parallel to the reference plane through the center of mass of the whole irregularly shaped body. The accuracy of this approximation has been investigated and results are summarized in Part 1. of this paper. In practical applications we assume that the gravity anomaly is due to the undulations of the depth of an interface between homogeneous layers with different densities such as e.g. the interface between the upper and lower Pannonian sediments or more often the interface of the sediments and the cristallyne basement. It also involves that there are no other inhomogeneities either horizontally or vertically (such as lateral variations in density or other interfaces corresponding to density changes). We also assume that the regional background has been properly removed, random variations have been smoothed.

The deepest point of the interface determines the depth of the horizontal reference plane. This will be considered the lower boundary of the causative body, while the upper boundary is defined by the interface. The gravity effect of horizontal and constant density layers is an additive

constant therefore the whole anomaly is due to the irregular ,,body" defined above.

The thickness of the body is usually no more than some hundred meters, and the average depth is not less than 1 km. It can be seen that in order to avoid side-effects the thickness have to be very small around the boundary of the investigated area or some additional procedure is necessary to overcome the disturbances of the side effects. We shall assume in the followings that the thickness and the average depth satisfy this requirements and call attention to that limitations the algorithm. All the assumptions should be checked in practical applications.

The undulations of the density contrast surface acts as a peculiar sheet-like body i.e. it is thin and large horizontally.

The gravity field due to a prism is approximated in turn by a mass point concentrated in the neighbourhood of its center.

Gravity anomalies due to various bodies are shown in Part 2. The accuracy of the double approximation is also dealt with in that part of the paper.

PART 1.

Approximation of the gravitational attraction due to a rectangular prism by that of a mass point in its center

The vertical component of the gravitational attraction of a rectangular prism is given by the integral

$$g(x, y, z,) = G \Delta g \int_{x-u_1}^{x-u_2} \int_{y-v_1}^{y-v_2} \int_{z-w_1}^{z-w_2} \frac{w}{[u^2+r^2+w^2]^{3/2}} \, du\, dv\, dw, \qquad (1.1)$$

where $g(x,y,z)$ denotes the vertical component of the field at the point x,y,z

G is the gravitational constant

$(6.67.10^{-8}$ cgs unit)

$\Delta\varrho$ is the density of the prism and

(u_1,v_1,w_1), $(u_1,v_1\, w_2)$, . . . (u_2,v_2,w_2)

are the coordinates of the corners of the prism and z is positive downwards.

The notations used in (1.1) are shown in *Fig. 1.1.* Various expressions were published for the integrated results (K e l l o g 1929, B o t e-

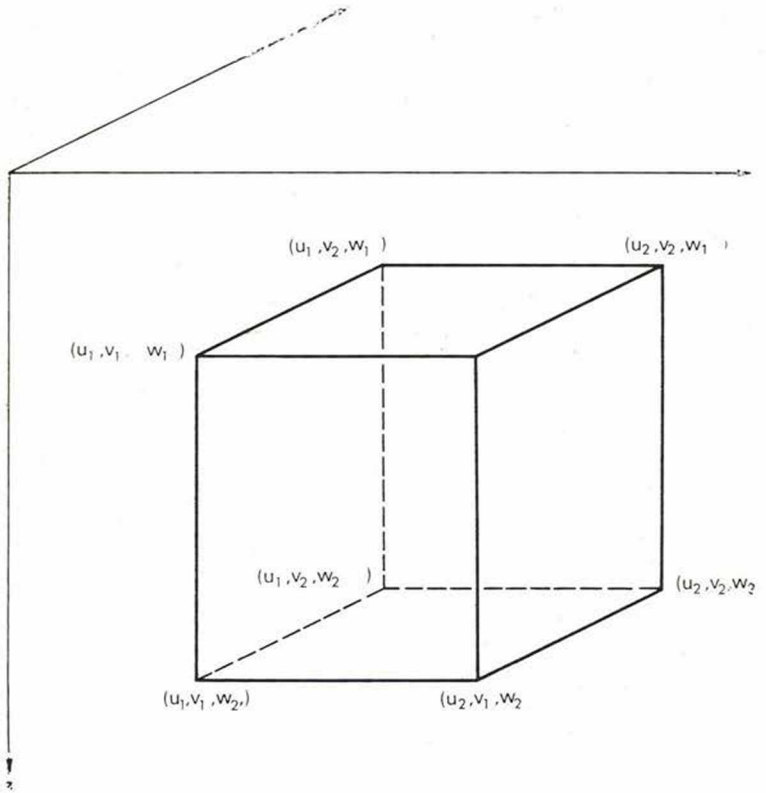

Fig. 1.1 Notations used in the derivation of the gravitational attraction of a rectangular prism

z a t u et. al 1971, N a g y, 1966 etc.) As G o o d a c r e (1973) pointed out a convenient from for $g\ (x,y,z)$ is

$$g(x,y,z) = G\,\Delta\varrho \left|\left|\left| u\ln(v+r) + v\ln(u+r) - w\,\mathrm{atan}\left(\frac{uv}{wr}\right) \right|\right|\right|_{x-u_1\ y-v_1\ z-w_1}^{x-u_2\ y-v_2\ z-w_2}, \quad (1.2)$$

where $r = (u^2+v^2+w^2)^{1/2}$

Equation (1.2) is an abbreviation for an expression consisiting of 8 terms. Before writing down the explicite version of the full expression let us introduce some notations. In practical applications $z = 0$ and the two other coordinates are integer multiples of the grid spacing; the latter be denoted by s, i. e.

$x = ks\ (k = -n,\ -n+1, \ldots 0, \ \ldots n-1,\ n)$ and

$y = ls\ (l = -m,\ -m+1, \ldots 0,\ m-1,\ m).$

The detailed expression for the z components of the gravity field in the point $(ks, ls, 0)$ is than

$$g(x, y, z) = G \Delta\varrho \sum_{i=1}^{8} t_i; \tag{1.3}$$

$$t_1 = (ks - u_2) \ln[ls - v_2) + r_1] + (ls - v_2) \ln[(ks - u_2) + r_1] + \\ + w_2 \operatorname{atan} \frac{(ks - u_2)(ls - v_2)}{-w_2 r_1}, \tag{1.4a}$$

$$t_2 = -\left[(ks - u_1) \ln[(ls - v_2) + r_2] + (ls - v_2) \ln[(ks - u_1) + r_2] + \right. \\ \left. + w_2 \operatorname{atan} \frac{(ks - u_1)(ls - v_2)}{-w_2 r_2}\right], \tag{1.4b}$$

$$t_3 = (ks - u_2) \ln[(ls - v_1) + r_3] + (ls - v_1) \ln[(ks - u_2) + r_3] + \\ + w_1 \operatorname{atan} \frac{(ks - u_2)(ls - v_1)}{-w_1 r_3}, \tag{1.4c}$$

$$t_4 = -\left[(ks - u_1) \ln[(ls - v_1) + r_4] + (ls - v_1) \ln[(ks - u_1) + r_4] + \right. \\ \left. + w_1 \operatorname{atan} \frac{(ks - u_1)(ls - v_1)}{-w_1 r_4}\right], \tag{1.4d}$$

$$t_5 = (ks - u_1) \ln[(ls - v_2) + r_5] + (ls - v_2) \ln[(ks - u_1) + r_5] + \\ + w_1 \operatorname{atan} \frac{(ks - u_1)(ls - v_2)}{-w_1 r_5}, \tag{1.4e}$$

$$t_6 = -\left[(ks - u_2) \ln[(ls - v_2) + r_6] + (ls - v_2) \ln[(ks - u_2) + r_6] + \right. \\ \left. + w_1 \operatorname{atan} \frac{(ks - u_2)(ls - v_2)}{-w_1 r_6}\right], \tag{1.4f}$$

$$t_7 = (ks - u_1) \ln[(ls - v_1) + r_7] + (ls - v_1) \ln[(kr - u_1) + r_7] + \\ + w_2 \operatorname{atan} \frac{(ks - u_1)(ls - v_1)}{-w_2 r_7}, \tag{1.4g}$$

$$t_8 = -\left[(ks - u_2) \ln[(ls - v_1) + r_8] + (ls - v_1) \ln[(ks - u_2) + r_8] + \right. \\ \left. + w_2 \operatorname{atan} \frac{(ks - u_2)(ls - v_1)}{-w_2 r_8}\right], \tag{1.4h}$$

where

$$r_1^2 = (ks-u_2)^2+(ls-v_2)^2+w_2^2 \tag{1.5a}$$

$$r_2^2 = (ks-u_1)^2+(ls-v_2)^2+w_2^2 \tag{1.5b}$$

$$r_3^2 = (ks-u_2)^2+(ls-v_1)^2+w_1^2 \tag{1.5c}$$

$$r_4^2 = (ks-u_1)^2+(ls-v_1)^2+w_1^2 \tag{1.5d}$$

$$r_5^2 = (ks-u_1)^2+(ls-v_2)^2+w_1^2 \tag{1.5e}$$

$$r_6^2 = (ks-u_2)^2+(ls-v_2)^2+w_1^2 \tag{1.5f}$$

$$r_7^2 = (ks-u_1)^2+(ls-v_1)^2+w_2^2 \tag{1.5g}$$

$$r_8^2 = (ks-u_2)^2+(ls-v_1)^2+w_2^2 \tag{1.5h}$$

Let us consider now the special case when the center of the prism is in the point (0,0,H) and therefore, the corners are given by

$$\left.\begin{aligned} u_1 &= -\frac{s}{2}, & u_2 &= \frac{s}{2} \\ v_1 &= -\frac{s}{2}. & v_2 &= \frac{s}{2} \\ w_1 &= H-\frac{h}{2}, & w_2 &= H+\frac{h}{2} \end{aligned}\right\} \tag{1.6}$$

which involves that the cross section of the prism is a grid square.

If we introduce the following abbreviations

$$\left.\begin{aligned} A_1 &= \left(k-\frac{1}{2}\right)s & A_2 &= \left(k+\frac{1}{2}\right)s \\ B_1 &= \left(l-\frac{1}{2}\right)s & B_2 &= \left(l+\frac{1}{2}\right)s \\ C_1 &= \left(H'+\frac{h'}{2}\right)s & C_2 &= \left(H'-\frac{h'}{2}\right)s \end{aligned}\right\} \tag{1.7}$$

where H' and h' are the depths of the mass center and the height of the prism, respectively, both measured in units of the grid spacing, the expressions (1.4a)–(1.4h) become

$$t_1 = A_1\ln(B_1+r_1)+B_1\ln(A_1+r_1)-C_1\,\mathrm{atan}\,\frac{A_1B_1}{C_1r_1}, \tag{1.8a}$$

$$t_2 = -\left[A_2\ln(B_1+r_2)+B_1\ln(A_2+r_2)-C_1\,\mathrm{atan}\,\frac{A_2B_1}{C_1r_2}\right], \tag{1.8b}$$

$$t_3 = A_1 \ln(B_2 + r_3) + B_2 \ln(A_1 + r_3) - C_2 \operatorname{atan} \frac{A_1 B_2}{C_2 r_3}, \tag{1.8c}$$

$$t_4 = -\left[A_2 \ln(B_2 + r_4) + B_2 \ln(A_2 + r_4) - C_2 \operatorname{atan} \frac{A_2 B_2}{C_2 r_4} \right], \tag{1.8d}$$

$$t_5 = A_2 \ln(B_1 + r_5) + B_1 \ln(A_2 + r_5) - C_2 \operatorname{atan} \frac{A_2 B_1}{C_2 r_5}, \tag{1.8e}$$

$$t_6 = -\left[A_1 \ln(A_1 + r_6) + B_1 \ln(A_1 + r_6) - C_2 \operatorname{atan} \frac{A_1 B_1}{C_2 r_6} \right], \tag{1.8f}$$

$$t_7 = A_2 \ln(B_2 + r_7) + B_2 \ln(A_2 + r_7) - C_1 \operatorname{atan} \frac{A_2 B_2}{C_1 r_7}, \tag{1.8g}$$

$$t_8 = -\left[A_1 \ln(B_2 + r_8) + B_2 \ln(A_1 + r_8) - C_1 \operatorname{atan} \frac{A_1 B_2}{C_1 r_8} \right], \tag{1.8h}$$

where

$$r_1^2 = A_1^2 + B_1^2 + C_1^2, \tag{1.9a}$$

$$r_2^2 = A_2^2 + B_1^2 + C_1^2, \tag{1.9b}$$

$$r_3^2 = A_1^2 + B_2^2 + C_2^2, \tag{1.9c}$$

$$r_4^2 = A_2^2 + B_2^2 + C_2^2, \tag{1.9d}$$

$$r_5^2 = A_2^2 + B_1^2 + C_2^2, \tag{1.9e}$$

$$r_6^2 = A_1^2 + B_1^2 + C_2^2, \tag{1.9f}$$

$$r_7^2 = A_2^2 + B_2^2 + C_1^2, \tag{1.9g}$$

$$r_8^2 = A_1^2 + B_2^2 + C_1^2. \tag{1.9h}$$

The computation of the z components of the gravity field of the rectangular prism having the corners (1.6) in a regular grid with spacing s can be performed according to the following scheme

a) determine the variables A_1, A_2, ... C_2 by equations (1.7)
b) computate the r_i values by equations (1.9)
c) evaluate formulas (1.8) i.e. calculate the t_i values
d) multiply the sum of the t_i–s by $G\varrho\Delta$. These steps are repeated for each (k, l) pairs.

The mass of the prism is

$$m = \Delta \varrho \, s^2 h$$

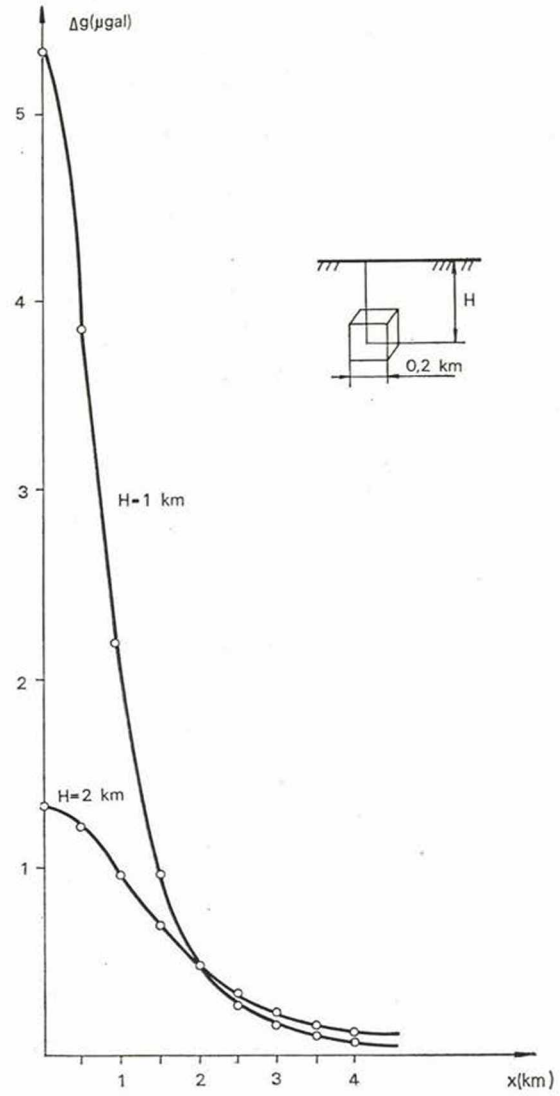

Fig. 2.2 Comparison between the z-components of the gravitational attraction due to cubes with edges of 0.2 km (empty circles) and that of mass points in their centers (continuous curves)

and because the center of mass lies in (O, O, H) the z component of the gravity field due to that mass, concentrated in the center becomes

$$g^*(ks, ls, 0) = G\,\Delta\varrho \frac{s^2\, h\, H}{[(ks)^2+(ls)^2+H^2]^{3/2}}$$

$$= G\,\Delta\varrho \frac{h'\, H'}{[k^2+l^2+(H')^2]^{3/2}} \qquad (1.10)$$

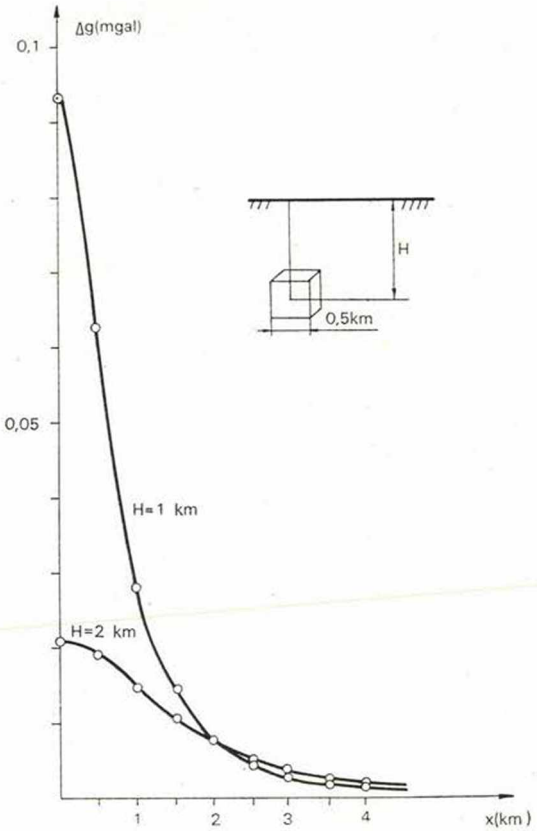

Fig. 1.3 Comparison between the z-components of the gravitational attraction due to cubes with edges of 0.5 km (empty circles) and that of mass points in their centers (continuous curves)

The goodness of fit between the exact field and its approximation (1.10) can be evaluated by direct comparison of the effects due to prisms with realistic parameters.

In those applications which are our main concern in Parts 2. and 3., H varies between 1 km and 2 kms while k is somewhere between 0 and 500 meters.

Figures 1.2 and *1.3* show the $g(ks, 0,0)$ values as empty circles for cubes with edges of 200 and 500 meters, respectively, in each case for two depths (1 km and 2 kms). The approximations obtained from the fields of mass points are drawn by continuous lines.

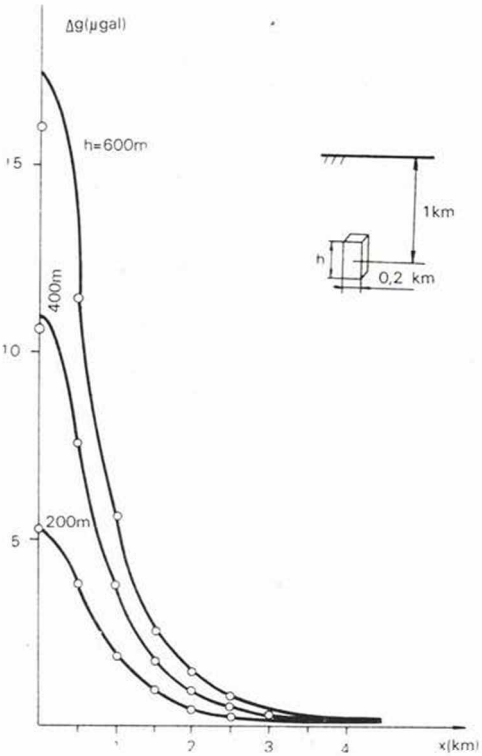

Fig. 1.4 Comparison between the z-components of the gravitational attraction due to rectangular prisms with $0{,}2 \times 0{,}2$ km^2 base and various height and that of mass points in their centers (continuous curves) when the depths of the mass centers are 1 km

Further exaples are shown in *Figs. 1.4* and *1.5*, where rectangular prisms have square cross sections with edges of 200 ms and heights of 200, 400 and 600 ms. The depths of the centers of masses are 1 km in *Fig. 1.4* and 2 kms in *Fig. 1.5*, respectively.

In all cases, shown as *Figs. 1.2* to *1.5*, the two-dimensional functions $g(x,y,0)$ and $g^*(x,y,0)$ are investigated along the x direction, only. This approach is justified if the field possesses circular symmetry. The field

due to a point source is indeed direction independent but the fields due to rectangular prisms are not. The largest deviations from gravity values along the direction of the x coordinate axis can be expected along the direction of the diagonal i.e. along the line $x = y$. The deviation from circular symmetry in the gravitational attraction of the prism can best be estimated by comparing the curves

$$g(x, y = 0, 0) \quad \text{and} \quad g(\sqrt{2}x, \sqrt{2}y, 0).$$

The directivity diminishes as the dimensions of the body decrease and the center of mass gets deeper therefore the worst situation which

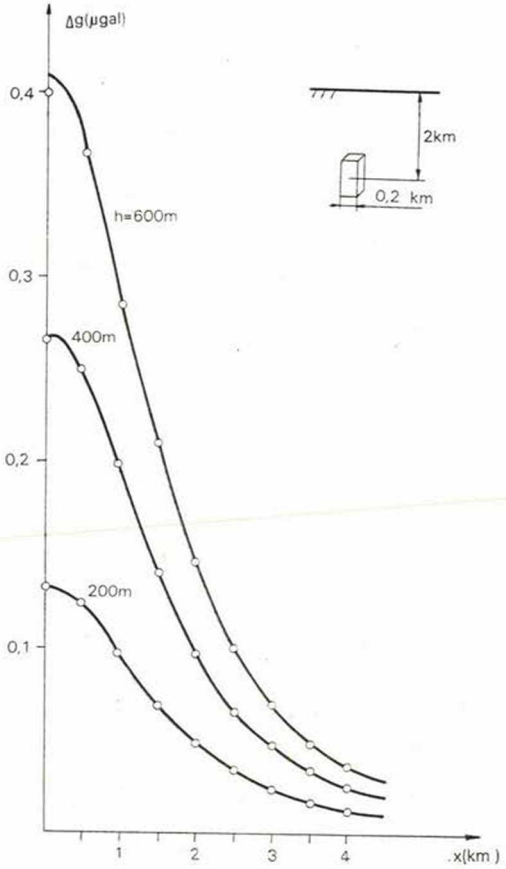

Fig. 1.5 Comparison between the z-components of the gravitational attraction due to rectangular prisms with $0{,}2 \times 0{,}2$ km^2 base and various heights and that of mass points in their centers (continuous curves) when the depths of the mass centers are 2 kms

has to be dealt with is that of the prism with $0{,}5 \times 0{,}5$ km^2 base and with center of mass at 1 km. Deviations for some situation are shown in *Fig. 1.7*. Numerical values were computed for various heights of the prisms along the directions $y = 0$ and $y = x$. The deviations, as it can be seen in *Fig. 1.7*, are very small. No values were found above 2 μgal which proves that the one-dimensional approach is justified. As a summary it may be said that the gravity field of an irregularly shaped body can be approximated by a sum of gravity fields due to point masses about the same accuracy as by a sum of gravity fields due to rectangular prism when the prisms are not larger than $500 \times 500 \times 500$ m^3 and the centers of masses lie in 1 km or deeper.

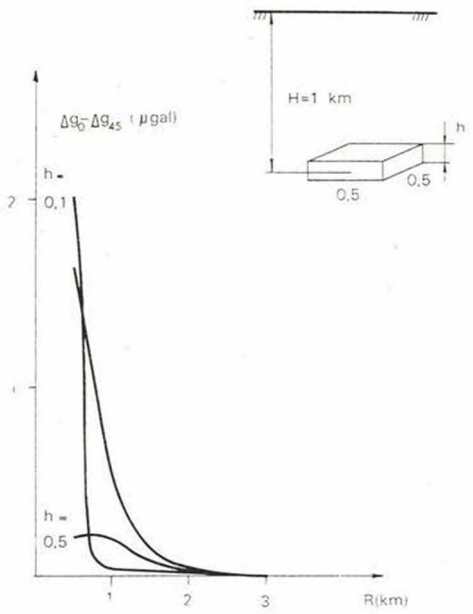

Fig. 1.6 Deviations between the z-components of the gravitational attraction measured along two profiles with directions 0° and 45°. The gravity fields are due to rectangular prisms with mass centers at 1 km and have a $0{,}5 \times 0{,}5$ km^2 square base and various thicknesses (denoted by h)

The economical advantage of the first approach is obvious because the computation of the gravity field due to a mass point is at least a hundred times faster. As a matter of fact the building up of the gravity field due to larger geological bodies or complicated surfaces from the field of rectangular prisms is really out of question when considering the limitations of our computational facilities.

Part 2.

Computation of the gravity field due to geological structures

Let us assume that the gravity anomaly field is solely due to the undulations of the interface between two homogeneous layers with different formation densities ϱ_1 and ϱ_2. The deepest point of the interface in the whole area defines the reference plane, the depth of which is denoted by H. (Notations are shown in *Fig. 2.1*). The mean depth of the interface will be denoted by H, the density contrast $\varrho_2 - \varrho_1$ by $\Delta\varrho$.

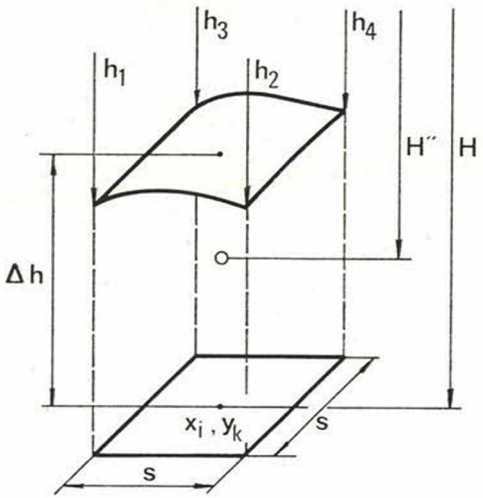

Fig. 2.1 To the computation of the gravity field due to a density interface

It is clear that the gravity anomaly caused by the undulations can be computed as the gravity effect of an irregular body bordered from below by the horizontal reference plane and otherwise by the interface and possesses a density $\Delta\varrho$. It is supposed that the interface reaches or comes close to the reference plane around the boundary of the area. We also assume that the mean depth is 1 km or more and the undulations around the mean depth do not exceed 0.3 km.

When the two latter assumptions are valid the body can be approximated by a bundle of rectangular prisms.

It is convenient to use the same rectangular grid system in the reference plane as the one determined by the observation points on the surface. The prisms therefore possess square bases. Observations are usually made at regular 0.5 km intervals in recent measurements, thus

the square basis are also of dimensions 0.5×0.5 km^2. In *Fig. 2.2* one of the prisms is shown (s stands for the grid interval). The heights of the prisms are estimated by

$$\Delta h_{ik} = H - \frac{h_1 + h_2 + h_3 + h_4}{4} \tag{2.1}$$

Where h_i denotes the depth of the interface in a grid point. (h_1, h_2, h_3 and h_4 are depths in the corners of a grid square). The mass of the prism is approximately

$$m_i = s^2 \Delta h \Delta \varrho \,. \tag{2.2}$$

The mass is then "concentrated" into a point with coordinates (x_i, y_k, H') where (x_i, y_k) is the center of the base and

$$H' = \frac{H + \overline{H}}{2} \,. \tag{2.3}$$

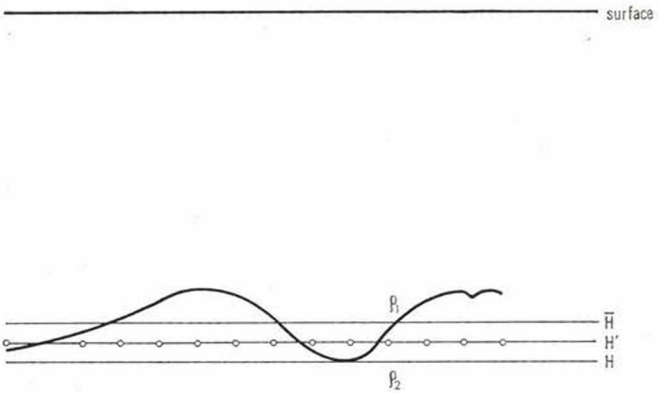

Fig. 2.2 Notations used in formulas (2.1) and (2.3)

The gravity effect of the prism is substituted by the effect of a mass point in (x_i, y_k, H') with mass determined by (2.2) i.e. the z-component of the gravity field in the point (u, v) is approximated by

$$g(u, v) = \frac{G \Delta\varrho \, \Delta h s^2 H'}{[(u - x_i)^2 + (v - y_k)^2 + (H')^2]^{3/2}} \,. \tag{2.4}$$

If the distances are given in kilometer units, $\Delta\varrho$ in $c.g.s$ units and $g_i(u, v)$ in mgals $G = 6.67$.

The gravity field due to the whole body is the sum of the individual fields each given by (2.4). When (u,v) is a point in a square grid $u = ms$; $v = ns$ and the coordinates x_i and y_k are also measured in units of the grid spacing the contributions from the prisms sums up to give

$$g(m,n) = 6{,}67 \sum_i \sum_k \frac{\Delta\varrho\, h_{ik} H''}{[(m-x_i')^2 + (n-y_k')^2 + (H'')^2]^{3/2}} \tag{2.5}$$

Where

$$H'' = \frac{H}{s},$$

$$x_i' = \frac{x_i}{s},$$

$$y_k' = \frac{y_k}{s},$$

Formula (2.5) can be thought of as a convolution between Δh_{ik} and

$$s(x_i, y_k) = \frac{H''}{[(x_i')^2 + (y_k')^2 + (H'')^2]^{3/2}} \tag{2.6}$$

$$x_i' = i + \frac{1}{2} \quad (i = -n,\ -n+1,\ \ldots,\ n-1);$$

$$y_k' = k + \frac{1}{2} \quad (k = -n,\ -n+1,\ \ldots,\ n-1).$$

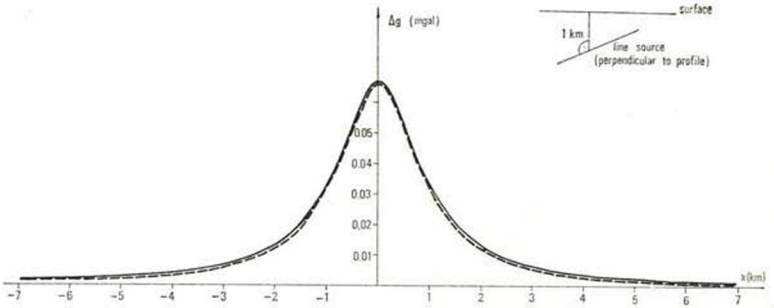

Fig. 2.3 Theoretical values of the gravity field of an infinite horizontal line source as measured along a profile perpendicular to the line (continuous curve) and its approximation obtained by (2.5) $y = 0$ (broken curve)

The accuracy of the proposed procedure has been checked by comparing gravity fields of simple bodies whose fields could have been expressed analytically to the gravity fields computed by (2.5). Some of the results are given in *Fig. 2.3–2.7*. *Fig. 2.3* shows the field of an infinite horizontal line source, buried at a depth of 1 km, along a line perpendicular to the body (continuous curve).

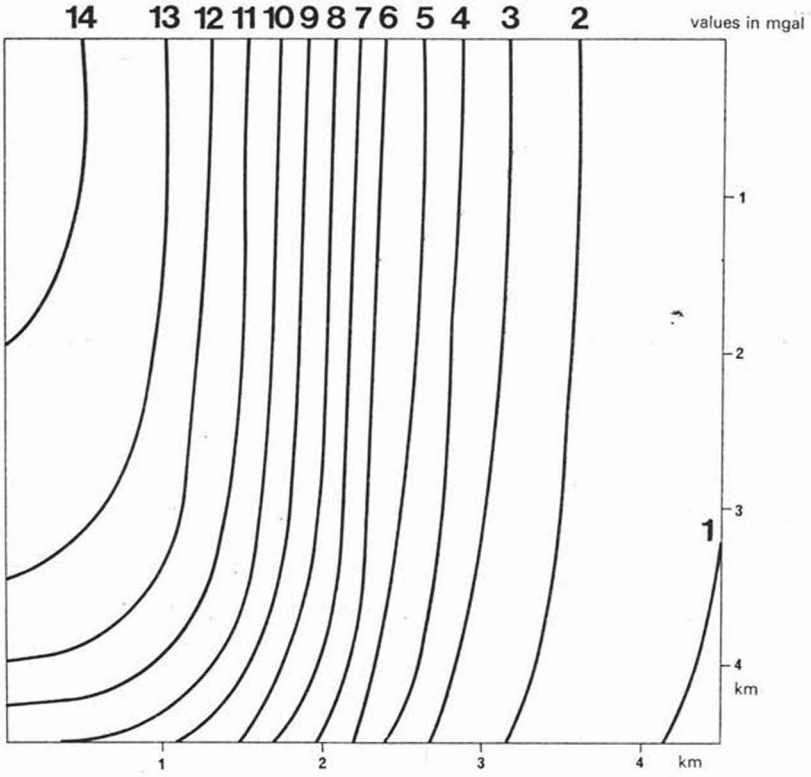

Fig. 2.4 The z-component of the gravity field due to a rectangular prism with dimensions $4\times10\times0{,}5$ km^2 with mass center at the depth of 1 km (exact formula) $\Delta\varrho = 1$ gcm^{-3}

The theoretical values come from the well known formula:

$$\Delta g(x) = 2G\,\lambda\frac{H}{H^2+\lambda^2}, \tag{2.7}$$

Where λ denotes the line density
and H is the depth.

The one dimensional modification of (2.5) gave the values connected by the broken curve in *Fig. 2.3.* The sampling distance was 0.5 km and 41 points were used to compute the convolution.

Fig. 2.4 shows the gravity field due to a rectangular prism whith dimension $4 \times 10 \times 0.5$ km^3, and with mass center at 1 km depth, as computed by the exact formulas (1.6) – (1.9).

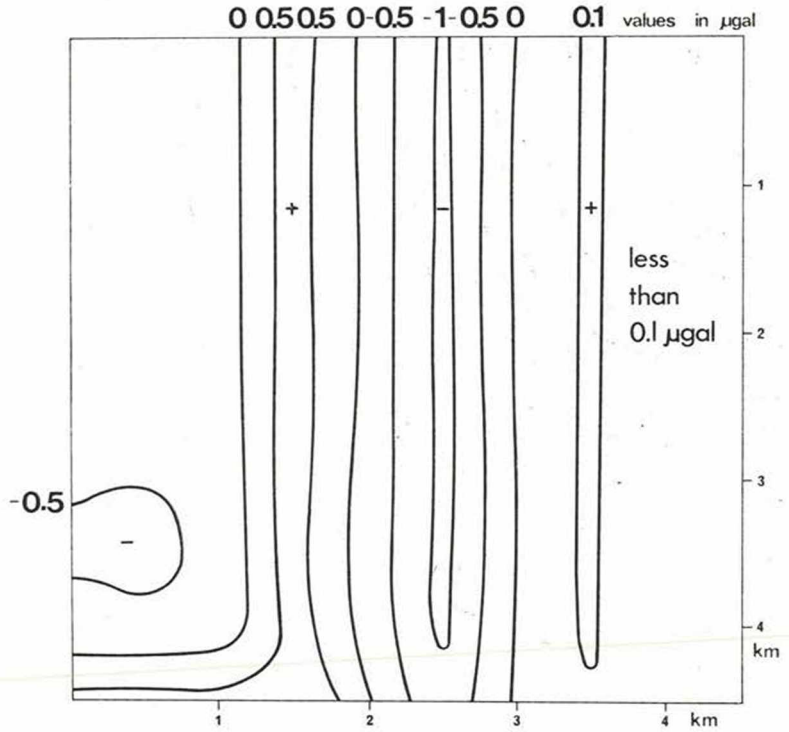

Fig. 2.5 Error field i.e. deviations between the theoretical gravity field shown in Fig. 2.4 and its approximation obtained by (2.5)

The convolution (2.5) gave a field so close to the theoretical one that the map, drawn from the approximate values is apparently identical to the "theoretical map" in *Fig. 2.4.* Therefore the difference field or "error field" has also been computed. Contours of the error field are shown in *Fig. 2.5.* We call the attention to the fact that the errors are given in 1μgal units and the isolines are 0,5μ gals apart. The deviations as indicated by the map can not be detected by the present measuring techniques.

Figs. 2.6 and *2.7* show similar quantities. *Fig. 2.6* is a field due to a $4 \times 4 \times 0.5$ km^3 rectangular prism at 1 km depth as computed according to the exact formulas while *Fig. 2.7* is the „error field" i.e. the difference of the theory and its approximation. The match of the convolution to the exact formula is excellent again. Numerous other models have been computed but the maximum of the deviations never exceeded 0.1 mgal for plausible geological models and $s = 0.5$ km sampling interval.

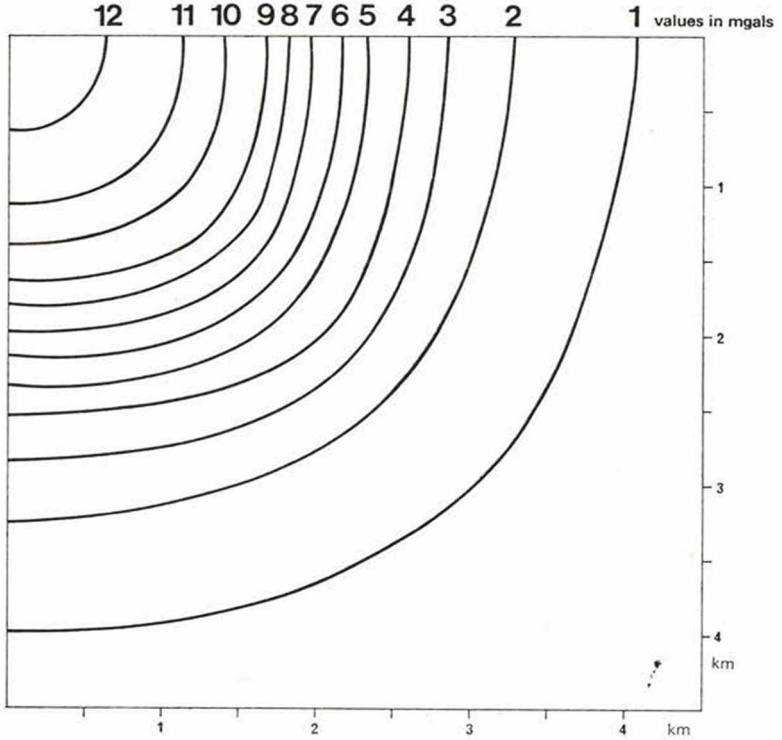

Fig. 2.6 The z-component of the gravity field due to rectangular prism with dimensions $4 \times 4 \times 0{,}5$ km^3 with mass center at the depth of 1 km (exact formula)

The application of equation (2.5) is further illustrated by *Fig. 2.8* and *2.9* where the gravity fields of a cone and a cylinder are shown respectively. On the upper parts of the figures the two dimensional fields are depicted by isolines on the lower part cross sections through the center of the models resp. the gravity fields are shown. The base

circle of the cone resp. the cylinder are drawn by broken lines. No comparison with theoretical values is possible because the gravity fields due to these bodies can not be expressed analitically.

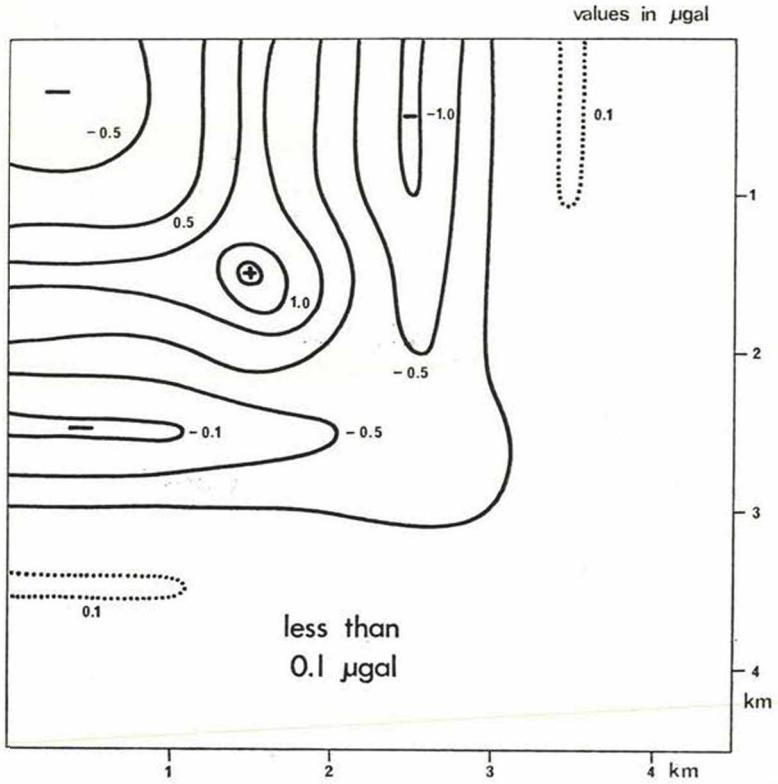

Fig. 2.7 Error field i.e. deviations between the theoretical gravity field shown in Fig. 2.6 and its approximation (the latter obtained by (2.5)).

The computation is rather fast and it does not need elaborate preparations as e.g. the method of T a l w a n i (1968) or storing and searching for the fields of appropriate cubes as the method proposed by B o t e z a t u et al (1973). It may therefore be of interest in itself. The simplified algorithm was developed in order to be able to solve the inverse problem by an iterative procedure in course of which the computation of the gravity fields due to geological models becomes necessary very often. Therefore our main concern had to be the speed and though some improvement of the algorithm can obviously be made (e.g. producing

denser spacing by interpolation, accurate positioning the center of mass for each prism etc.) but only at the cost of computer time. The approximation being satisfactory as it is now, we shall not deal with the improvement of the accuracy of the direct problem in this paper.

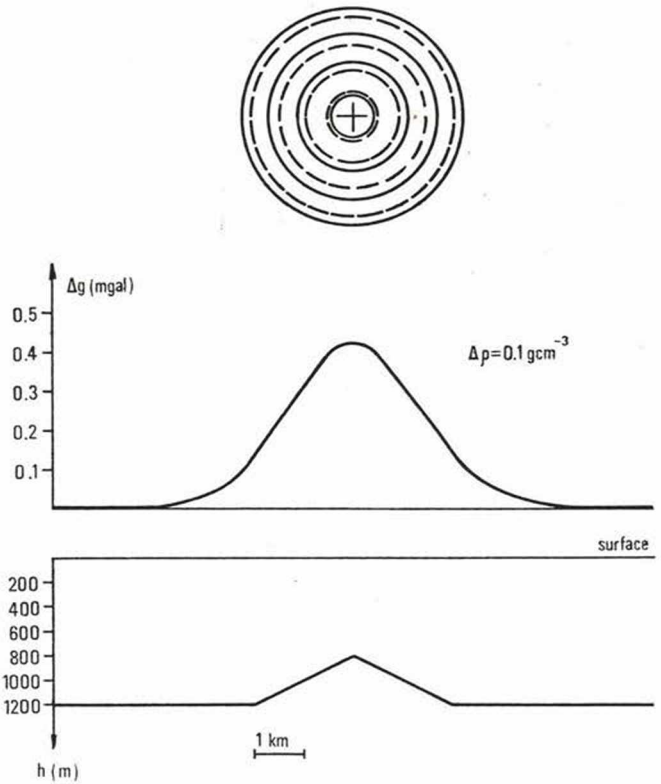

Fig. 2.8 The z-component of the gravity field due to a cone. Two-dimensional representation (upper part) and a profile through the center (lower part)

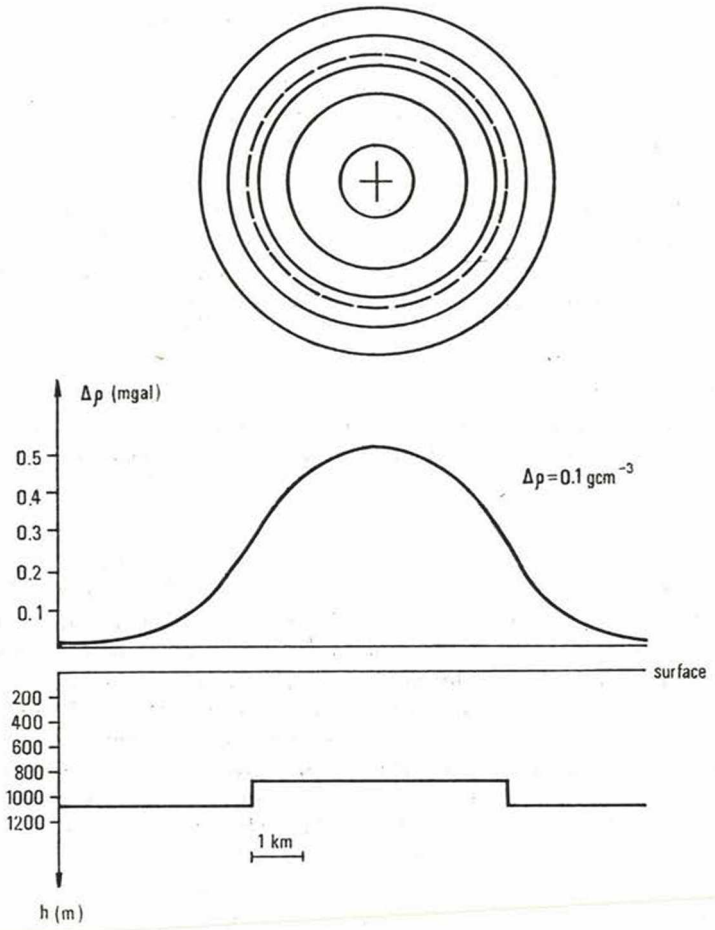

Fig. 2.9 The z-component of the gravity field due to a cylinder. Two-dimensional representation (upper part) and a profile through the center (lower part)

PART 3.

The iterative solution of the inverse problem

The inputs of the iteration are the measured gravity anomaly digitized in a square grid, the depth of the reference plane and the density contrast $\Delta\varrho$. As it has been mentioned in the previous sections it is assumed that the regional and random noise have been removed (or attenuated as much as possible) and therefore the anomaly is supposed to be due to the undulations of the density contrast surface alone.

The lower boundary of the causative body is the reference plane the upper boundary is the undulating interface.

The causative body is approximated by vertical prisms each having a cross section of one grid square and a thickness given by the average of the four vertical distances between the interface and reference plane in the corners of the grid square.

The density of the prisms is equal to the density difference between the two layers i.e. $\Delta\varrho = \varrho_2 - \varrho_1$.

The iterative process consits of setting a starter model for the thicknesses h_{ik}, computing the gravity field due to the model by the method described in Part 2. and modify the thicknesses in a way which diminishes the differences between the measured data (i.e. the input) and the computed data. Let us denote the thicknesses in the j-th iterative step by $h_{ik}^{(j)}$ and the measured and calculated gravity data by $g_{ik}^{(m)}$ and $g_{ik}^{(c)}$, respectively. The caculated data are functions of the thicknesses

$$g_{ik}^{(c)} = f[h_{ik}^{(j)}]. \tag{3.1}$$

The explicit form of the connection is described by (2.5). We have to find the best fit between $g_{ik}^{(m)}$ and $g_{ik}^{(c)}$. The goodness of fit can be expressed by various measures e.g. by the mean square deviation or by the sum of the absolute values of the deviations or by the largest error etc. None of them yields a feasible algorithm for the computation of the unknown parameters. Theoretically (3.1) can be rewritten in the form of simultaneous equations and this would unambigously determine all the h_{ik} values, but the solution of simultaneous equations with some hundred unknows is such a tremendous task that this way obviously should be abandoned.

Some heuristic approach is needed, which allows the fast determination of the h_{ik}-s and is able to improve the values in successive approximations. The chosen measure of the goodness of fit is then used only to check whether the new approximation is better than the previous and when a certain limit is reached it may be used to terminate the process. When $g_{ik}^{(c)}$ is greater than $g_{ik}^{(m)}$ it obviously means that the thicknesses in and around the grid point P_{ik} should be diminished. Though the $g_{ik}^{(c)}$ is a sum of various contributions from all prisms the greatest contribution comes from the prism vertically beneath that grid point. Therefore we modify the thickness of that prism by

$$K(g_{ik}^{(m)} - g_{ik}^{(c)}) = \Delta h_{ik}^{(j)} \tag{3.2}$$

where K is a constant multiplier the choice of whose numerical value will be dealt with later. The starter model may also be constructed by using this consideration. If the gravity field at the grid point P_{ik} would be

solely due to the prism vertically beneath and this is concentrated to a mass point lying in the mean depth H', g_{ik} would be

$$g_{ik} = \frac{G\, h_{ik}\, s^2\, \Delta\varrho}{(H')^2}\,. \tag{3.3}$$

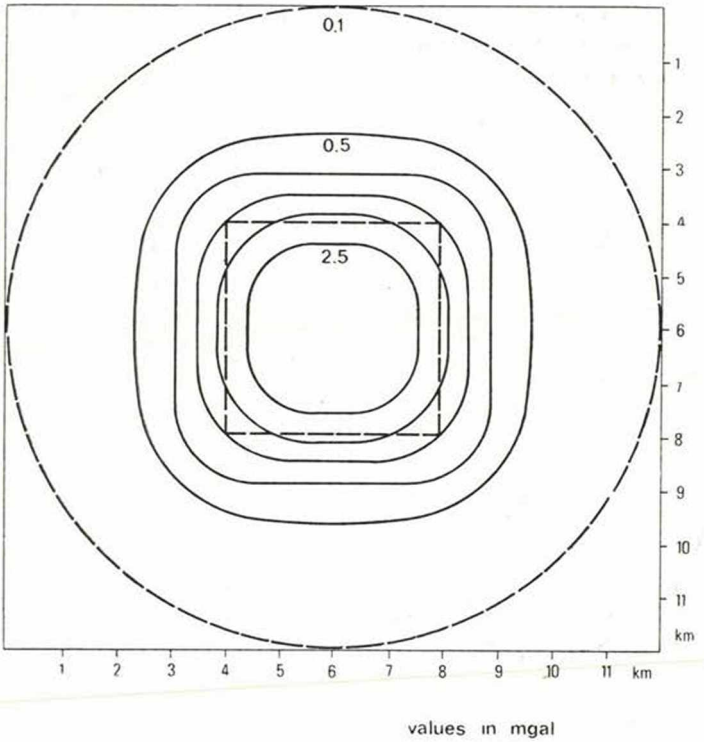

Fig. 3.1 The z-component of the gravity field due to a thin rectangular prism with base of 5×5 km^2 and height 0,1 km. Density contrast is 0.1 cgs unit. Values of the field over an area of 21×21 km^2 were used as input to the iterative process

From that equation follows

$$h_{ik}^{(o)} = \frac{g_{ik}}{f\,\Delta\varrho}\left(\frac{H'}{s}\right)^2 = \frac{g_{ik}}{0{,}667}\,(H'')^2 \tag{3.4}$$

when g_{ik} is measured in mgals and $h_{ik}^{(o)}$ in kilometers. This choice is different from that suggested in the literature e.g. by B o t t (1960) or by

Cordell and Henderson (1968). They used the Bouguer slab formula i.e.

$$h_{ik}^{(o)} = \frac{g_{ik}}{2\pi G \Delta\varrho}. \tag{3.5}$$

It can be shown, however, that the starter models (3.4) and (3.5) are very similar, both giving thicknesses proportional to the gravity data. The starter model is used to compute the first set of $g_{ik}^{(c)}$ data and equation (3.2; gives the first set of corrections to the starter model i.e. in this and in all the following steps

$$h_{ik}^{(j+1)} = h_{ik}^{(j)} + \Delta h_{ik}^{(j)}. \tag{3.6}$$

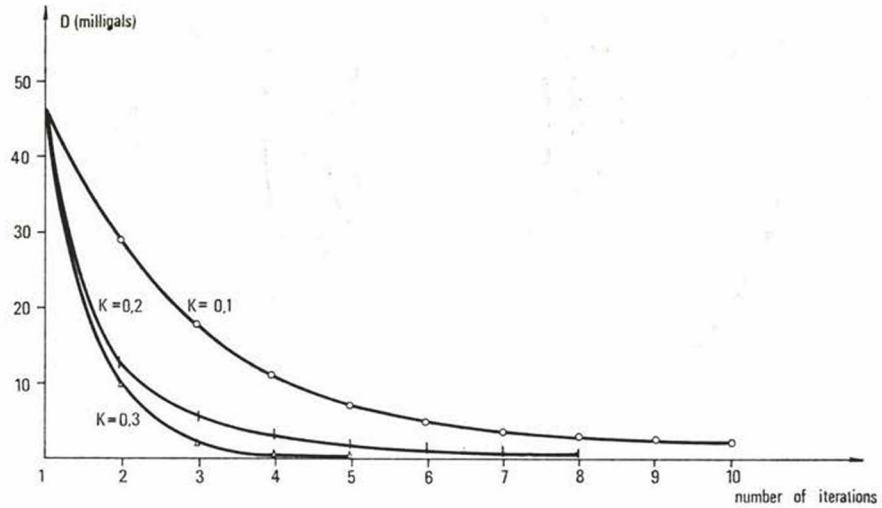

Fig. 3.2 Deviations between exact and computed values, represented by the first absolute moments (formula 3.7) plotted against the number of iterations for three values of the parameter

The gravity field due to the model with the „improved thicknesses" is computed by the approximations described in Part 2. The computed $g_{ik}^{(c)}$ values are input to equation (3.2) yielding new corrections to be applied again in equation (3.6).

The sum of the absolute values of the differences are also computed in each step. The process terminates when

$$D = \sum_{i,\,k} \left| g_{ik}^{(m)} - g_{ik}^{(c)} \right| \leq 0{,}001\, N \quad \text{(mg als)} \tag{3.7}$$

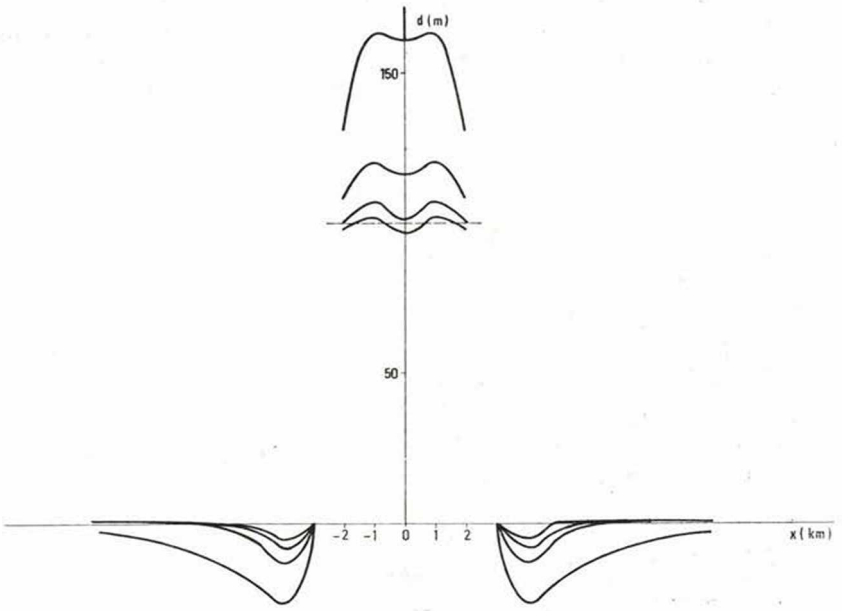

Fig. 3.3 Variation of the calculated cross sections of the structure obtained in iterative steps

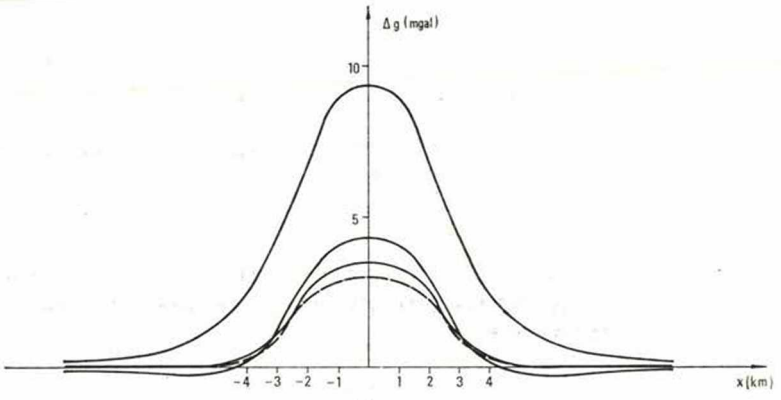

Fig. 3.4 Variation of the calculated gravity field along a profile in the iterative steps

where N is the number of grid points. Equation (3.7) involves that the measured and calculated fields are considered identical when the average difference is less than 0.001 mgal. It is not proved that the iterative process converges but in all cases investigated so far rather fast convergence have been found.

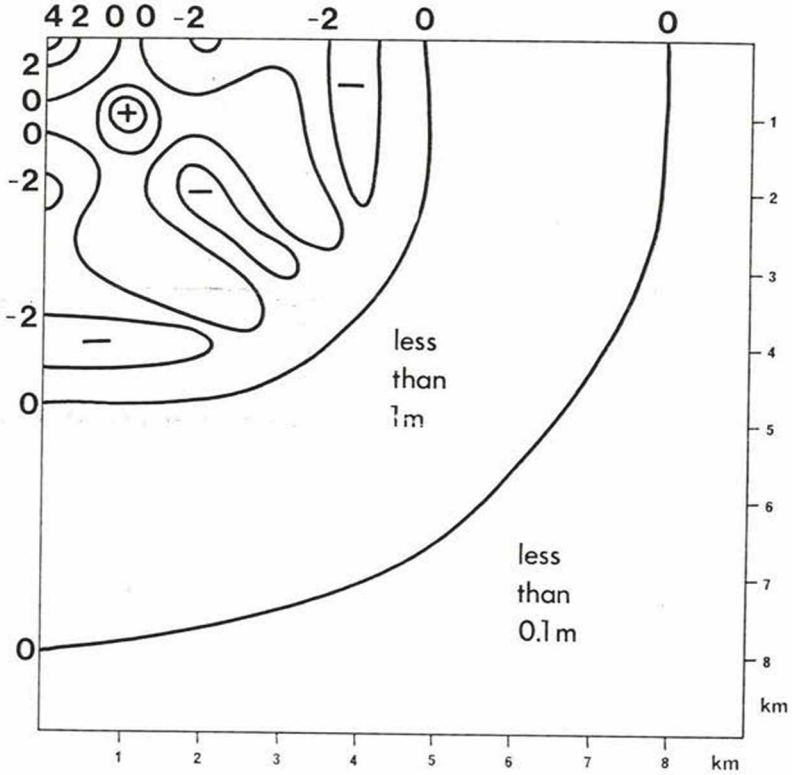

Fig. 3.5 The map of the deviations between the model structure and its last approximation

A method described by C o r d e l l and H e n d e r s o n (1968. p. 597) uses the following defining relationships between thicknesses in two consecutive iterative steps

$$h_{ik}^{(j+1)} = \frac{g_{ik}^{(m)}}{g_{ik}^{(c)}} h_{ik}^{(j)}. \tag{3.8}$$

(Instead of the denotations of the cited publication we used those defined in this paper for a better comparison.) The convergence of Cordell and Hendersons procedure is slower that the convergence obtained by (3.4) and (3.6) by a factor about 2 depending on the properties of the geological test model.

A further disadvantage of equation (3.8) is that it can not be modified when necessary while equation (3.4) contains a parameter K which may also be used to influence the speed of convergence.

Fig. 3.1. through *3.4* illustrate both the application of the present procedure and the role of the parameter K.

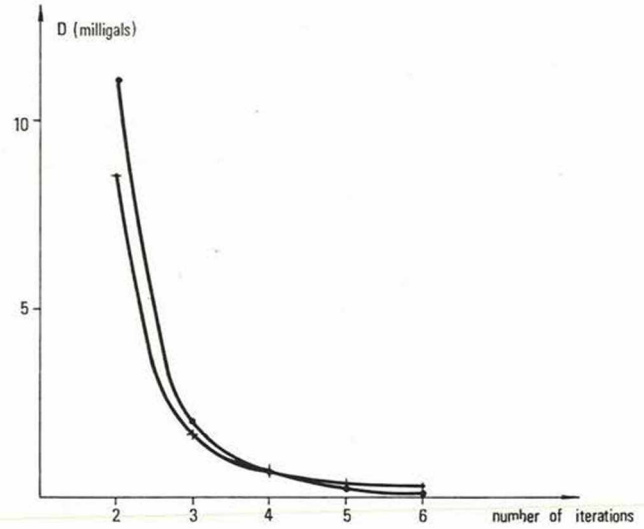

Fig. 3.6 The variation of the D (first absolute moment) if the depth of the reference plane has a 10% error (continuous line) the variation of D for the exact depth is also shown for a comparison (broken line)

The test structure is a thin rectangular prism with a square horizontal cross section. The edges of the prism are 5 km, 5 km and 0.1 km. The depth of the reference plane is 1 km, the density contrast $\Delta\varrho = 0.1$ cgs unit. The gravity field produced by the test model is shown in *Fig. 3.1* over an area of 21×21 km^2. The field was digitized and input to the iterative procedure. It would be cumbersome and superfluous as well to show all intermediate results for various K values and in each iterative steps. *Fig. 3.2* illustrates rather clearly the role of K by showing the D (defined by the left hand side of (3.7)) plotted against the number of iterations. If

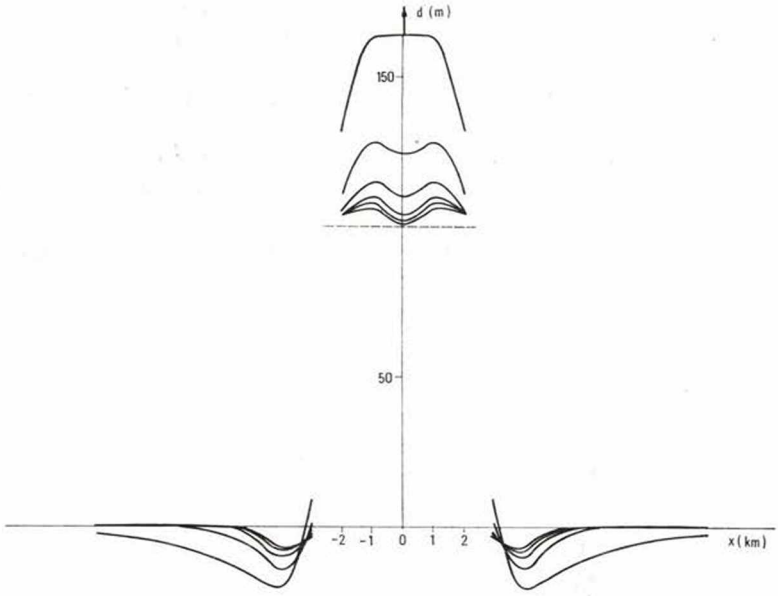

Fig. 3.7 Calculated cross sections of the structure obtained in the iterative steps if the depth of the reference plane has a 10% error

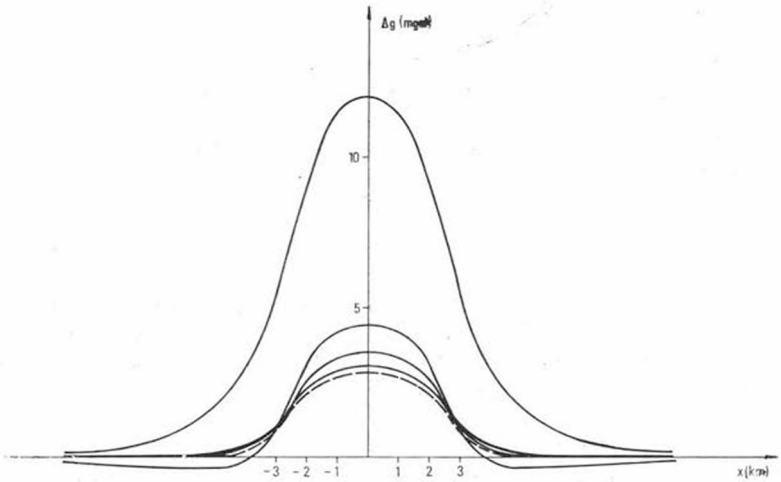

Fig. 3.8 Calculated gravity fields along a profile in the iterative steps if the depth of the reference plane has a 10% error

$K = 0.1$ convergence is slow. With $K = 0.2$ the process become faster but some improvement is desirable. $K = 0.3$ proved to be the proper choice. In order to give an idea of the variations of the computed structure and its calculated gravity field in the consecutive iterations vertical cross sections are shown in *Fig. 3.3.* and *3.4* respectively. The section goes through the center of the structure (and therefore through the center of the gravity field). It is worth to mention that while the computed

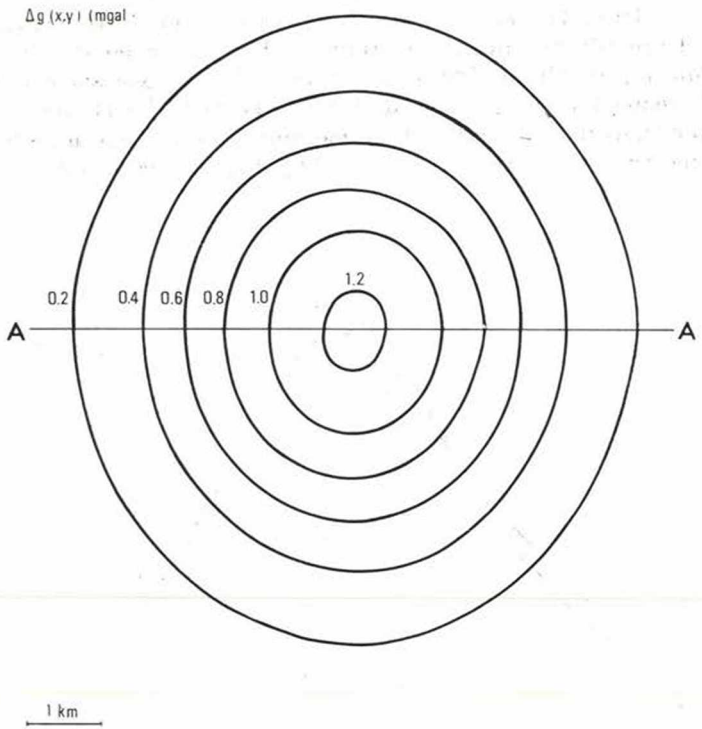

Fig. 3.9 Gravity field due to a realistic geological structure. The place of a profile is indicated by straight line A – A'

gravity field becomes appearently identical with the measured field the computed structure deviates from the model. The errors i.e. the deviations between the model and the computed structures are shown by isolines in *Fig. 3.5.* Similar map for the deviations between ,,measured" and computed gravity fields is not worth to construct because deviations are smaller than 0.005 milligal everywhere. The errors in the computed struc-

ture are not due to the computational method but may be considered as due to the limited "resolving power" of gravity field measurements. Undulations of order of some meters at about the depth of 1 km can not be detected at the surface.

It may be of interest that a slight change in the depth of the reference plane gives a solution whose field is also very close to the field of the model and the convergence of the iterations remains rather fast. The speed of convergence is illustrated by a plot of D values against the number of iterations shown in *Fig. 3.6.* The similar quantities obtained by the use of the exact depth are also shown for a comparison. It would be difficult to say from the speed of convergence which is the correct depth. Cross sections illustrating the change in the calculated structure and the corresponding gravity fields in the iterative steps are shown in *Fig. 3.7.* and *3.8*, respectively. As it might be expected the structure seems to be thicker than it is in reality because more anomalous mass is necessary to produce the same gravity effect if the depth becomes greater.

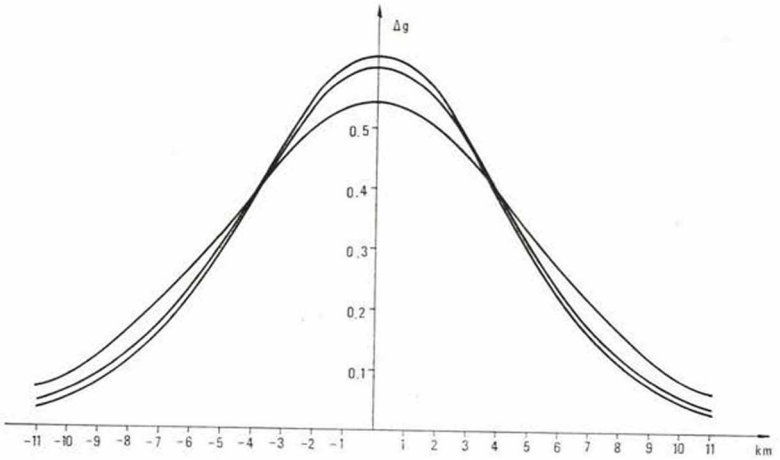

Fig. 3.10 Calculated cross sections of the structure obtained in iterative steps

The gravity field of a realistic structure is shown in *Fig. 3.9.* Results of the iterations are illustrated by data along a profile through the peak of the structure. Some of the calculated cross sections and the calculated gravity values are shown in *Fig. 3.10.* and *3.11.* The exact values are So close to the last iteration that separate lines could not be drawn. The illustrations show that the iterative process converges very rapidly and the obtained values are very close to the model structure.

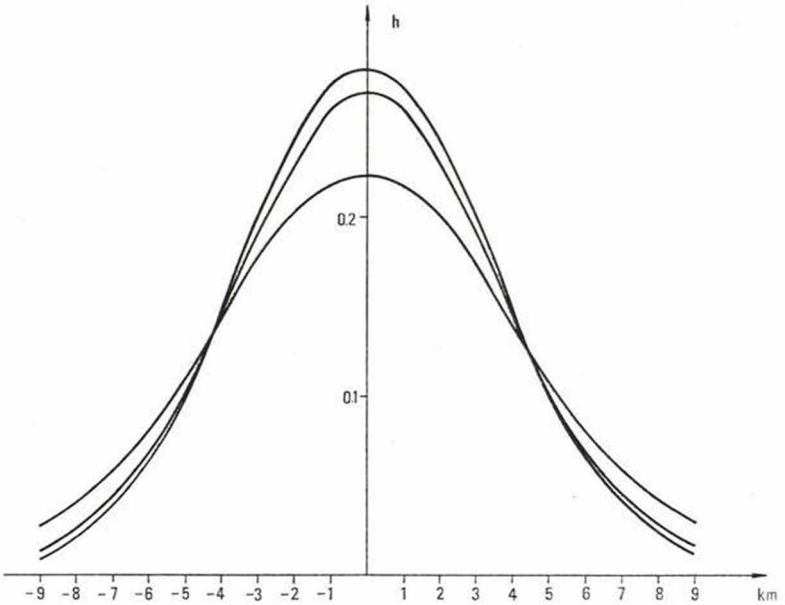

Fig. 3.11 Calculated gravity values along the profile in the iterative steps ($\triangle$g values should be multiplid by 2)

REFERENCES

A l - C h a l a b i, M. (1971): Interpretation of gravity anomalies by non-linear optimization. Geophysical Prospecting, Vol. 20. p. 1 – 16.

B o t e z a t u, R., V i s a r i o n, M., S c u r t u, F. and C u c u, G. (1971): Approximation of the gravitational attraction of geological bodies. Geophys. Prosp. Vol. 19. pp. 218 – 227.

B o t t, M. M. P. (1960): The use of rapid digital computing methods for direct gravity interpretation of sedimentary basin. Royal Astronomical Soc. Geophys. Jour. Vol. 4. No 1. p. 63 – 67.

C o r d e l l, L. and R. G. H e n d e r s o n, (1968): Iterative three-dimensional solution of gravity anomaly data using a digital computer. Geophysics. Vol. 33. No 4. p. 596 – 601.

G o o d a c r e, A. K. (1973): Some comments on the calculation of a homogeneous rectangular prism. Geophys. Prosp. Vol. 21. pp. 66 – 69.

K e l l o g g, O. D. (1929): Foundations of potential theory Julius Springer, Berlin.

N a g y, D. (1966): The gravitational attraction of a right rectangular prism. Geophysics, Vol. 31. p. 362 – 371.

T a l w a n i, M. and M. E w i n g (1960): Rapid computation of gravitational attraction of threedimensional bodies of arbitrary shape. Geophysics, Vol. 25. No 1. p. 203 – 225.